ELSEVIER

Contents lists available at ScienceDirect

Food Research International

journal homepage: www.elsevier.com/locate/foodres



Phage-loaded alginate films and coatings for biofilm inhibition and control in food packaging

Fernanda Coelho ^{a,b,*}, Larissa Ribas Fonseca ^c, Lorenzo Pastrana ^b, Sanna Sillankorva ^{b,**}, Valtencir Zucolotto ^a

- a Nanomedicine and Nanotoxicology Group (Gnano), São Carlos Institute of Physics, University of São Paulo, São Carlos, São Paulo, Brazil
- ^b International Iberian Nanotechnology Laboratory, Portugal
- ^c Department of Food Engineering and Technology, School of Food Engineering, University of Campinas, São Paulo, Brazil

ARTICLE INFO

Keywords: Food packaging Biofilm Antimicrobial efficacy Phages

ABSTRACT

Food packaging plays a crucial role in ensuring food safety; however, microbial contamination, particularly from biofilm-forming bacteria, remains a challenge. This study explores the use of sodium alginate-based films and coatings loaded with a bacteriophage cocktail targeting Escherichia coli and Pseudomonas fluorescens to mitigate biofilm formation in food packaging, with a focus on cheese products. The coatings were applied to parchment paper, polystyrene, and films prepared with sodium alginate loaded with bacteriophages, and assessed for their antimicrobial efficacy. Biofilm inhibition and control experiments were performed by applying phage-containing films/coatings either immediately after bacterial inoculation or after 24 h of biofilm formation. Samples were then incubated and analyzed for viable cells, biomass, metabolic activity, and live/dead bacterial ratio. Phageinfused films and coatings demonstrated significant antimicrobial activity, effectively reducing biofilm biomass. Biofilm inhibition experiments were more pronounced in phage-loaded films, achieving up to a 1.7-log reduction in viable cells and a 70.8 % decrease in biomass for E. coli, as well as a 2.7-log reduction in viable cells and a 66.62 % decrease in biomass for P. fluorescens. In biofilm control experiments, the phage-loaded materials also exhibited inhibitory effects, with a maximum CFU reduction of 1.39 logs compared to the untreated control for P. fluorescens and 0.72 logs compared to the untreated control for E. coli in films. Biomass reduction reached 42 % for E. coli films and 19 % for P. fluorescens films. Confocal microscopy and COMSTAT analysis confirmed a reduction in biofilm thickness and a significant decrease in live bacterial cells in treated samples. When applied to cheese, phage-loaded materials maintained strong antimicrobial activity over 24 h, with parchment paper achieving log reductions of 2.5 and 2.3 compared to the untreated control for P. fluorescens and E. coli, respectively. These findings highlight the potential of phage-infused alginate coatings as promising strategies for active food packaging.

1. Introduction

Food packaging plays a central role in the food industry, influencing product quality, safety, and consumer perception (Sharma et al., 2023). One of its greatest challenges is the control of microbial contamination, a critical factor for ensuring food safety and extending shelf life (Papadochristopoulos et al., 2021).

A major contributor to contamination in the food chain is the presence of biofilm-forming bacteria. These microorganisms adhere to

surfaces, persist in processing environments, and compromise product quality and safety, leading to spoilage, reduced shelf life, and potential health risks (Milho et al., 2018). The growing demand for fresh, minimally processed foods and their global distribution amplifies these risks, while the economic burden associated with biofilm-related losses further underscores the need for innovative antimicrobial strategies (Sharan et al., 2022).

Biofilms are particularly problematic in dairy processing. A variety of bacterial species, each with distinct growth requirements, can

E-mail addresses: fernanda.coelho1408@gmail.com (F. Coelho), sanna.sillankorva@inl.int (S. Sillankorva).

^{*} Corresponding author at: Nanomedicine and Nanotoxicology Group (Gnano), São Carlos Institute of Physics, University of São Paulo, São Carlos, São Paulo, Brazil.

^{**} Corresponding author.

colonize surfaces and persist throughout the production chain (Bremer & Seale, 2009). Contamination may occur even before milk enters processing facilities, revealing critical vulnerabilities. Although pasteurization is effective against many pathogens, thermoduric and thermophilic bacteria, including spore-forming Bacillus spp., can survive heat treatment and remain a persistent issue (Gopal et al., 2015). Similarly, thermotolerant *Escherichia coli* strains and biofilm-associated contamination in bulk tank milk have been reported (Hammad et al., 2022). *Pseudomonas fluorescens*, one of the most common milk contaminants, is often linked to inadequate water quality and hygiene during processing, resulting in sensory defects in dairy products (Eneroth et al., 2000; Kumar et al., 2019).

Within the dairy sector, cheese represents a product of particular concern. Global cheese production continues to grow, driven by consumer demand for healthier, natural products and the diversity of flavors, textures, and forms it offers. However, cheese surfaces are highly susceptible to microbial contamination due to favorable pH and high water activity (Proulx et al., 2017). Packaging therefore plays a decisive role in maintaining quality during storage and transport, protecting cheese from physical damage, environmental conditions, and microbial spoilage (Berti et al., 2019).

To meet these demands, technologies such as modified atmosphere packaging (MAP), vacuum packaging, and active packaging have been widely applied, enabling shelf-life extension while reducing the need for chemical additives (Singh & Nalwa, 2011). Nevertheless, the use of synthetic, non-biodegradable films raises environmental concerns, reinforcing the importance of sustainable alternatives. A promising strategy is the integration of established preservation techniques with biobased packaging materials, thus combining effective food protection with reduced ecological impact.

In this context, biological antimicrobial agents incorporated into packaging are gaining prominence. These natural compounds offer targeted action, lower reliance on synthetic additives, and compatibility with eco-friendly materials (Wagh et al., 2023). Among them, bacteriophages stand out as innovative, selective bioadditives capable of controlling bacterial pathogens in food systems. Recently, our group developed a phage cocktail incorporated into sodium alginate matrices, producing films and coatings on parchment paper and polystyrene via ultrasonic spray coating, which showed promising results for food packaging applications (Coelho et al., 2025). Although alginate films are fully biobased, their use as coatings on conventional plastics highlights the trade-off between functionality and sustainability.

Recent studies have increasingly explored the incorporation of bacteriophages and other biocontrol agents into edible and biodegradable matrices, highlighting their potential to inhibit biofilm formation and enhance food safety (Dhulipalla et al., 2025; Figueiredo et al., 2021; García-Anaya et al., 2023). For instance, Cui et al. (2017) demonstrated that chitosan coating incorporated with a phage-loaded nanoliposomes effectively reduced Escherichia coli on ready-to-eat meats, while Costa et al. (2023) reported synergistic antimicrobial effects using alginatebased nanocomposites in dairy applications. Despite these advances, most investigations have focused on planktonic bacteria or singlematerial systems, often neglecting the comparative performance between coatings and free-standing films under realistic food storage conditions. Furthermore, comprehensive biofilm evaluation combining metabolic, structural, and imaging analyses remains scarce. This study addresses these gaps by integrating multiple quantification methods and assessing functional performance in actual cheese matrices, thereby advancing the current understanding of phage-based biopackaging systems.

The present study advances this line of research by comprehensively evaluating bacteriophage-loaded sodium alginate coatings and films against biofilm-forming bacteria relevant to the dairy industry. Unlike most previous studies focused on planktonic cells, here we assess biofilm inhibition and control through complementary methods, including colony counts, biomass quantification, metabolic activity, and confocal

laser scanning microscopy with COMSTAT analysis. Furthermore, by comparing coatings and free-standing films, we emphasize their distinct advantages: coatings offer a practical solution to modify existing packaging, while films represent standalone, biodegradable alternatives to synthetic plastics. Finally, the evaluation of these materials in cheese samples under realistic storage conditions strengthens the translational relevance of this work by bridging laboratory findings with practical applications in the food industry.

2. Materials and methods

2.1. Materials

Alginic acid sodium salt and the sodium chloride were acquired from Sigma-Aldrich (Portugal). Glycerol 99.5 % (ν/ν) was purchased from Alfa Aesar (USA), Tris base and PEG 8000 were purchased from Fisher BioReagentsTM (USA), calcium chloride and MgSO4 from Panreac Applichem (Spain). Tryptic Soy Broth (TSB): Corning® (USA), Tryptic Soy Agar (TSA): Hardy Diagnostics, CriterionTM line (USA) Crystal Violet (reagent grade): Carolina Biological Supply (USA), CHROMagarTM Orientation: CHROMagar (France), Resazurin (sodium salt): Biotium (USA); also available from R&D Systems – Bio-Techne (USA). SYTO 9 and Propidium Iodide (PI): included in the LIVE/DEAD BacLight Bacterial Viability Kit, Thermo Fisher Scientific (USA).

2.2. Bacteria and phages

Pseudomonas fluorescens ATCC 27663 and Escherichia coli BL21 (Invitrogen, Thermo Fisher Scientific) were used as host strains for bacteriophage isolation. Cultures were maintained at 37 °C in tryptic soy broth (TSB) or on TSB solid medium (TSB supplemented with 1.5 % (w/v) agar).

The bacteriophages employed in this study had been previously isolated and characterized (Coelho et al., 2025). The *Pseudomonas* phage FSB24 belongs to the Studiervirinae subfamily, genus Pifdecavirus, while the *Escherichia* phage North is classified within the family Straboviridae, genus Krischvirus. These phages differ in plaque morphology and replication traits, with phage FSB24 forming larger plaques (3.4 \pm 0.6 mm) and exhibiting a higher burst size (142.2 \pm 39.1 PFU/infected bacterium) compared to phage North (0.78 \pm 0.01 mm, 60.5 \pm 4.1 PFU/infected bacterium).

Both phages were incorporated into sodium alginate solutions to produce antimicrobial films and coatings, which were prepared as previously described (Coelho et al., 2025).

2.3. Films and coatings

Films and coatings were prepared following Coelho et al., 2025. An antimicrobial sodium alginate solution (1–2 % w/v) was incorporated with Pseudomonas phage FSB24 and Escherichia phage North ($\sim 10^7$ PFU/mL) under stirring. The same volume of this solution was used for both preparation approaches to ensure an equivalent initial phage load per sample area. For film formation, 20 mL of solution was cast onto 9.2 cm Petri dishes and dried at 30 °C for 24 h. Dried films were cross-linked by immersion in 0.2 % (w/v) CaCl₂ containing phages ($\sim 10^8$ PFU/mL) for 5 min, followed by drying at 30 °C for 24 h, resulting in films 30–34 μ m thick. For coatings, parchment paper and polystyrene substrates were treated using an ultrasonic spray coater, where ten layers of the same alginate–phage solution were applied and subsequently cross-linked with CaCl₂. The coatings showed thicknesses of approximately 51 μ m on parchment paper and 69 μ m on polystyrene. Controls included films and coatings without phages, as well as uncoated substrates.

2.4. Time kill assay

The Clinical & Laboratory Standards Institute (CLSI) M26-A protocol

was followed to perform time-kill assays (Barry et al., 1999). Briefly, each bacterial culture, *P. fluorescens* and *E. coli* (1 mL, 5×10^8 CFU/mL), was separately diluted in 9 mL of TSB. Then, 100 µL of the corresponding phage suspension (5×10^9 PFU/mL) or 100 µL of SM buffer (control) was added. The mixtures were incubated at 30 °C (120 rpm) for *P. fluorescens* and 37 °C (120 rpm) for *E. coli*. Samples were collected at 0, 1, 3, 5, 7, and 24 h post-infection. Serial 10-fold dilutions of *P. fluorescens* and *E. coli* cells were prepared in saline solution containing 10 mM ferrous ammonium sulfate. Three independent experiments were performed in triplicate.

2.5. Phage release

To assess the phage release profile from sodium alginate films and coatings, round samples (1 cm diameter) were placed in 500 μ L of SM buffer under continuous agitation at room temperature (22 °C). Samples were collected at designated time points to evaluate phage release. The quantity of released phage particles was determined by counting plaqueforming units (PFU).

2.6. Biofilm inhibition and biofilm control experiments

Pre-inocula of P. fluorescens and E. coli were prepared in TSB and incubated overnight at 30 °C and 37 °C, respectively. The overnight cultures were then diluted 10⁶-fold in fresh medium, and ten microliters of this dilution were added onto 0.2 µm pore-size membranes placed on TSA agar to mimic biofilm formation. This membrane-based model is widely used to simulate biofilm development on solid supports, offering a standardized and reproducible setup that facilitates quantitative and microscopic analyses (Han & Lee, 2023). Biofilms of P. fluorescens were formed at 30 °C, while biofilms of E. coli were formed at 37 °C, with both incubations lasting 24 h. The two experiments performed differ in the time the films/coatings were applied. For the biofilm inhibition experiments, after inoculation of the membranes with bacteria, these were immediately exposed to the phage containing films/coatings and incubated for 24 h. After incubation, the samples were processed for viable colony quantification (CFU), biomass quantification (crystal violet (CV)), metabolic activity assays (resazurin) and visualized in CLSM to determine the live/dead bacterial ratio. For the biofilm control experiments, the membranes were inoculation as above and incubated for 24 h to allow the formation of biofilm. After, films/coatings were applied, and the samples were incubated for an additional 24 h before the quantification of CFU, CV and metabolic activity. Films and coatings devoid of phages were used as controls for both experiments.

2.6.1. Assessment of biofilm viable cells by colony count

After the respective incubation times for evaluating inhibition (24 h) and control (48 h) of biofilms under the influence of films and coatings, the treatments were removed, and the membranes containing the biofilm were transferred to microtubes. Next, 1 mL of PBS solution was added to the microtubes, and the biofilm cells were resuspended by vigorous pipetting. The suspended biofilm was then transferred to a new flat-bottom 96-well microplate, followed by the preparation of tenfold serial dilutions in PBS. Five 10-µL drops of each dilution were plated onto agar media corresponding to the broths used for biofilm production (e.g., PIA for *Pseudomonas* biofilm and ChromAgar Orientation for *E. coli*). Colony-forming units (CFU) were enumerated after 24 h of incubation at 37 °C. The experiment was performed twice, with three replicates each.

2.6.2. Assessment of biofilm biomass by crystal violet

Biofilm biomass measurements were performed using crystal violet (CV) staining. After the biofilm incubation period, the membranes were carefully removed and transferred to a 96-well plate. Each well received 190 μL of a 0.1 % aqueous CV solution (Sigma-Aldrich), followed by incubation at room temperature for 30 min. To remove excess dye, the

wells were washed three times with sterile distilled water. Subsequently, $30\,\%$ acetic acid solution was added to each well to solubilize the bound dye, and the plate was incubated at room temperature for $15\,$ min. Absorbance was measured using a microplate reader at $595\,$ nm and $530\,$ nm, respectively. The readings provided quantitative data on biofilm biomass based on dye retention. The experiment was performed twice, with three replicates each.

2.6.3. Assessment of metabolic activity of biofilm cells by resazurin

A resazurin solution (Sigma-Aldrich) was prepared at a concentration of 16 µg/mL in sterile PBS. For the assay, the membrane containing the biofilm was carefully transferred to a 96-well plate and washed with 200 µL of PBS. Subsequently, 100 µL of the diluted resazurin solution were added to each biofilm-containing well, along with their respective negative controls. The microplates were incubated in the dark at 30 °C and 37 °C for 2 h. A multimode microplate reader (Varioskan LUX, Thermo Fisher Scientific) was used to measure relative fluorescence units (RFU) (λ Ex 530 nm and λ Em 590 nm) after incubation. The experiment was conducted twice, with three replicates each.

2.6.4. Assessment of biofilm thickness and live/dead bacterial ratio using confocal microscopy to analyze

Membrane samples with biofilm and different treatments were used for evaluation by confocal microscopy. For fluorescent staining of bacteria, the live/dead BacLight-Bacterial Viability Kit 7012 (Invitrogen, Mount Waverley, VIC, Australia) was used. The stain is composed of two fluorophores, SYTO9 (green) and propidium iodide (PI; red), which are capable of detecting membrane integrity. PI is typically used to identify dead cells in a population and SYTO9 for live cells. The excitation/emission maxima for these dyes are about 480/500 nm for SYTO9 staining and 490/635 nm for propidium iodide. After staining the samples according to the manufacturer's protocol, biofilm formation was analyzed using a confocal laser scanning microscope (CLSM; Zeiss LSM 780 Confocal Microscope, Zeiss, Jena, Germany). Biofilm coverage at four random locations at each site. The Zeiss ZEN Microscope Software version 3.0 was used for generation of orthogonal and 3D images.

2.6.5. COMSTAT analysis

The 3D quantification of biofilm was carried out using COMSTAT 2.1 (www.comstat.dk) (Heydorn et al., 2000; Vorregaard, 2008). Three merged image stacks were used to get statistical difference. The number of images in each z-stack varied depending upon the thickness of the biofilm. The pixel and voxel values were set after calibrating the images by correlating the image pixel dimensions with the physical measurements in ImageJ. The z-stack images were converted to 8-bit and saved in OME-TIFF format through ImageJ to process through COMSTAT. A threshold setting of the image stacks was carried out after visual examination. A fixed threshold value of 20 was applied to all the image stacks. Connected volume filtering was used to remove biofilm patches that were not attached to the substratum. Several biofilm parameters such as biomass, maximum thickness, average thickness (biomass), roughness coefficient, and surface to volume ratio were calculated.

2.6.6. Antimicrobial activity of bacteriophage-loaded sodium alginatebased films and coatings in cheese sample

The antimicrobial activity assay was conducted in accordance with ISO 22196, with minor adaptations. Cheese pieces (Parmigiano Reggiano) were purchased from a local supermarket and aseptically cut into smaller portions measuring $5\times 5~cm^2$, with an average weight of 14.5 ± 2.81 g. To reduce background bacterial levels prior to inoculation, the samples were irradiated with UV-C light for 30 min (15 min per side). Each cheese portion was then uniformly inoculated over the entire surface with 100 μL of either *P. fluorescens* or *E. coli* suspensions ($\sim \! 10^5$ CFU/cm²). Sodium alginate-based films and coatings containing phages were cut into $5\times 5~cm^2$ pieces and carefully placed in direct contact with the inoculated cheese surface. Samples were incubated at 22 °C for 7

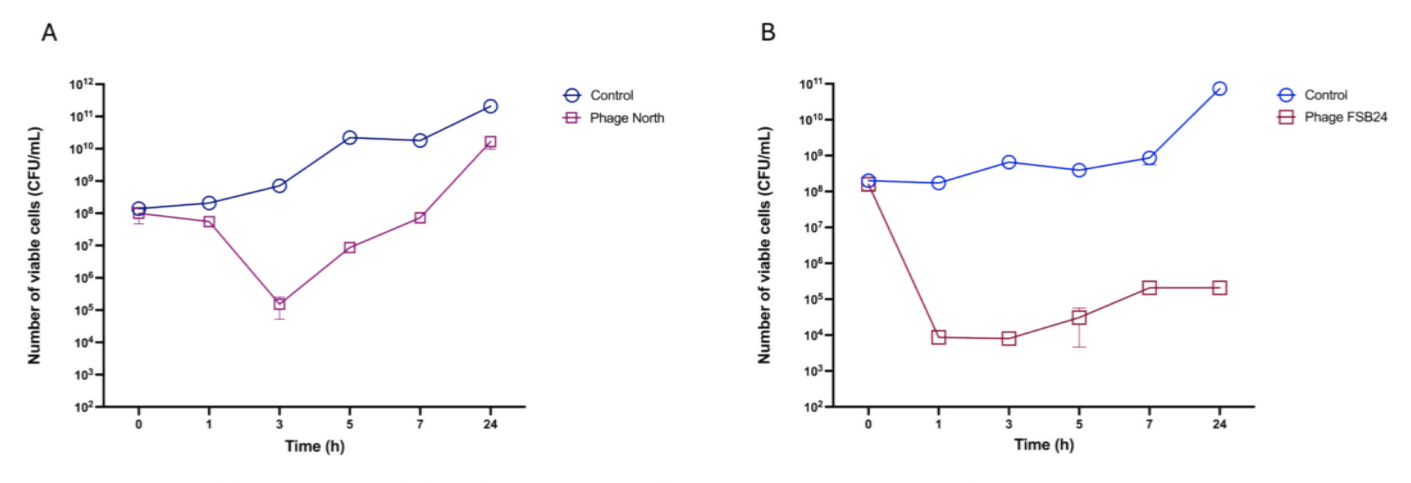


Fig. 1. Time-kill experiment of each phage alone. (A) phage North, MOI of 10, 120 rpm, 37 °C. (B) phage FSB24, MOI of 10, 120 rpm, 30 °C.

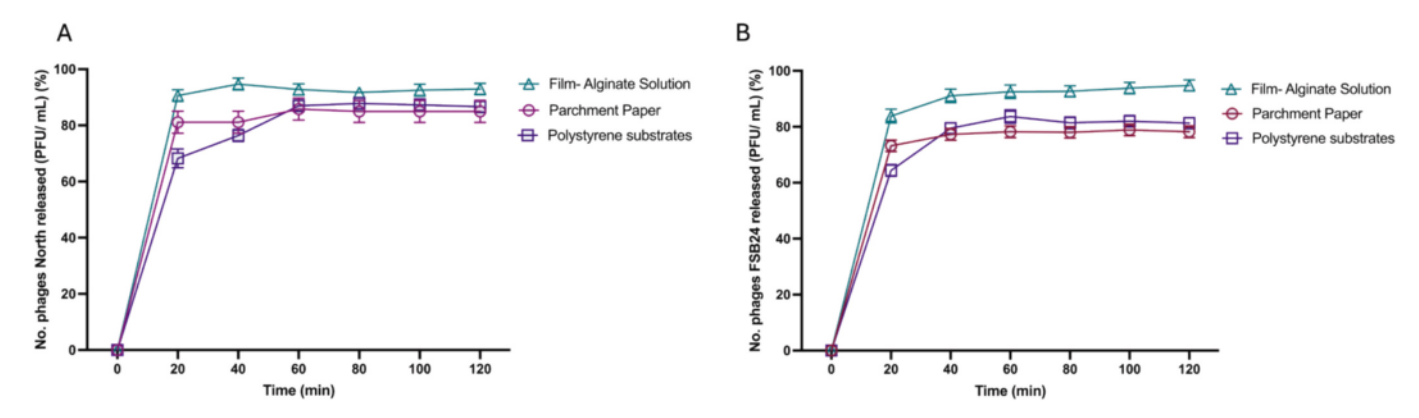


Fig. 2. Phage release in different materials. A and B show the release profiles of phages from film, paper and plastic substrates over time. (A) focuses on phages North, while (B) illustrates phages FSB24.

days, while sodium alginate-based films and coatings without phages served as controls. Representative images of the experimental setup (cheese coverage with film and coating) are provided in the Supplementary Material for clarity.

After 24 h and 7 days, the samples were aseptically transferred to sterile Falcon tubes, and tenfold serial dilutions were prepared in saline solution. The resulting suspensions were plated on Petri dishes containing PIA medium for P. fluorescens and ChromAgar Orientation medium for P. verification of the coli. Plates were incubated overnight at 30 °C and 37 °C, respectively, and CFU counts were subsequently performed.

2.7. Statistical analysis

Statistical analysis was conducted using the analysis of variance (ANOVA) method, and Tukey's test for mean comparison was performed using Statistica software for Windows (version 12, StatSoft Inc., Tulsa, OK, USA). A p-value of less than 0.05 was deemed statistically significant.

3. Results and discussion

In this study, the antimicrobial efficacy of bacteriophage-loaded sodium alginate-based films and coatings was evaluated through a series of assays, including time-kill kinetics, biofilm inhibition and control, and application on cheese samples.

3.1. Time kill assay

The efficacy of these two phages was assessed through time-kill

experiments (Fig. 1).

Time-kill experiments revealed that the phage North achieved a 3.7 log CFU/mL reduction (Fig. 1A) within 3 h. However, regrowth of $\it E.~coli$ cells was observed after 3 h post-infection, with only a 1.1 log CFU/mL reduction sustained after 24 h. In contrast, phage FSB24 exhibited superior antibacterial activity, reducing bacterial counts by 4.3 log CFU/mL within 1 h and the bacterial levels were maintained 5.5 log CFU/mL lower for up to 24 h compared to the control (Fig. 1B).

3.2. Phage release

Phage release assays were performed to compare the release profiles across different groups (Fig. 2). The results show that the release kinetics for both phages are similar across the three materials. For all samples, there is an initial burst release followed by a stabilization.

The theoretical phage concentration was set at 100 % for both phages, and the release from the films closely matched this value, whereas an underestimation was observed for the coatings. The release from the films was approximately the same for both phages (94.66 % for the North phage and 94.77 % for the FSB24 phage). In contrast, the release from the other two matrices was lower. The release from polystyrene paper varied between 83 % (phage FBS24) to 87.81 % (phage North) and from parchment paper between 79 % (phage FSB24) and 86 % (phage North). One possible reason for this reduced release could be phage loss due to deposition at of the sodium alginate solution containing phages in areas outside the intended substrate area.

Phage release from films and coatings plays a critical role in protecting food products from bacterial contamination by allowing phages to interact with their bacterial targets. Our findings align with the

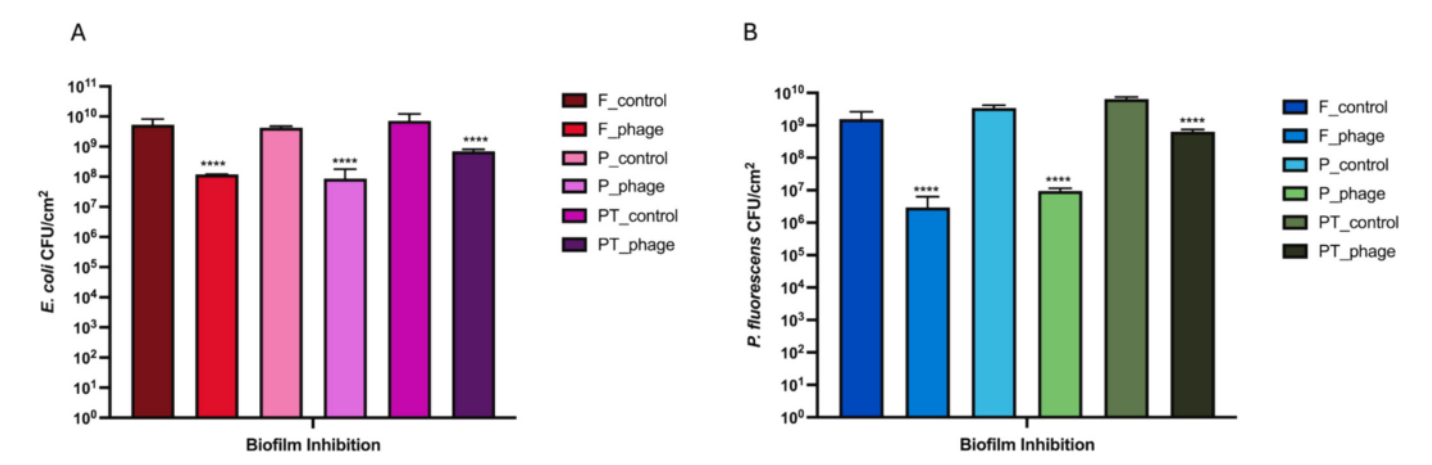


Fig. 3. Viable cell counts (CFU/mL) of *E. coli* (A) and *P. fluorescens* (B) after 24-h inhibition assays on different materials. F_control: Film without phages; F_phage: Film with phage cocktail; P_control: Parchment paper without phages; P_phage: Parchment paper with phage cocktail; PT_control: Polystyrene without phage cocktail; PT_phage: Polystyrene with phage cocktail. Bars represent the mean CFU/mL with error bars indicating standard deviation. ****: P < 0.0001.

literature, showing rapid phage release in the initial hours. For instance, Alves et al. (2019) suggested that phage release from films depends on factors like phage size and film swelling capacity. They assessed the release of φ IBB-PF7A phage from sodium alginate films, where phage-loaded films were placed in SM buffer with continuous stirring at 4 °C. Aliquots taken at intervals revealed that most phages were released within the first 2–3 min.

Building upon these insights, the present study further explores the role of film composition in modulating phage release. As previously observed in the characterization of the physical properties of alginatebased films (Coelho et al., 2025), the hydrophilic nature and solubility of these films play a crucial role in the dynamics of phage diffusion. The films crosslinked with 0.2 % (w/v) CaCl₂, which exhibited complete solubility in the earlier study, now demonstrate an accelerated phage release profile, reinforcing the role of moisture exposure in facilitating diffusion. While a controlled and sustained release would indeed be advantageous for long-term preservation, the rapid release observed in this study can be beneficial in specific food applications. In particular, ready-to-eat or refrigerated products are often most vulnerable to contamination during the early stages of storage and handling. A fast and effective release ensures that a high number of active phages are immediately available to interact with potential bacterial contaminants, thereby providing a strong initial antimicrobial effect. This early protection is especially relevant for foods with shorter shelf lives or those consumed within a few days, where rapid antimicrobial action outweighs the need for sustained release.

Similarly, Radford et al. (2017) observed high phage release rates, with levels reaching up to 99.9 % from xanthan gum coatings. In their study, the *Salmonella* phage Felix 01 and the *Listeria* phage A511 phages were incorporated into xanthan gum coatings at a concentration of 9 log PFU·cm² and applied to meat. Results showed over 99.9 % of both phages were released from the meat samples within 30 min at both 4 °C and 10 °C, demonstrating effective phage delivery for antimicrobial purposes. In comparison, the present study with sodium alginate-based films and coatings demonstrated similarly high release rates, with complete diffusion occurring within 60 min due to their rapid solubilization. Both studies highlight the effectiveness of polysaccharide-based coatings in delivering phages quickly, achieving a near-total release in a short time frame.

3.3. Biofilm inhibition experiments

Both bacteria are known biofilm formers where *P. fluorescens* takes advantage of its high motility due to its polar flagella being able to evenly colonize surfaces (Kumar et al., 2019). On the other hand, *E. coli*

is less motile due to its peritrichous flagella relying on cell-cell aggregation to form biofilms (Kamdar et al., 2023). Biofilm inhibition is thus an important characteristic that antimicrobial packaging should possess. Therefore, the inhibition efficacy of the developed films and coatings was evaluated by determining the viable cells, biomass, metabolic activity of the phage-loaded samples and compared to the controls.

3.3.1. Assessment of biofilm viable cells by colony count

Overall, both *E. coli* and *P. fluorescens* colonize the matrices in relevant numbers. Despite *P. fluorescens* better motility, with *E. coli* reaching slightly higher numbers than *P. fluorescens*. This is explained by the faster growth rate of *E. coli* (The specific growth rate is approximately 2.80 h⁻¹, and the doubling time is around 15 min) compared to *P. fluorescens* (The specific growth rate is 1.93 h⁻¹, and the doubling time is approximately 21.56 min. All phage loaded films and coatings present antimicrobial activity compared to the control samples. For *E. coli*, the best antimicrobial effect was observed with phage-loaded films (1.7-log10 CFU/cm² reduction), and the worse effect was obtained for polystyrene which showed a 1.02 log decrease compared to the control (Fig. 3A). Phage FSB24 proved to be more effective than phage North in inhibiting the growth of the respective bacterial host achieving reductions in the range of 1.01log10 CFU/cm² (polystyrene) to 2.7 log10 CFU/cm² (films) (Fig. 3B).

The inhibition results for E. coli align with the 24-h kill-time assay for phage North, which showed a 1.1-log reduction after 24 h. However, for phage FSB24, although inhibition was observed, it did not reach the strong antimicrobial activity (5.5-log reduction) seen in the kill-time assay. This discrepancy may be due to differences in experimental conditions. The time-kill assays are performed in liquid culture, where the rotation during incubation may enhance phage adsorption to the host (Sillankorva et al., 2008), particularly in the case of P. fluorescens. In contrast, in biofilm inhibition experiments, once a phage lyses a bacterium, the infection cycle may be limited if new susceptible hosts are not within reach. Additionally, bacterial growth on surfaces promotes the production of extracellular polymeric substances (EPS) (Simões et al., 2007), which encase the bacteria and may obscure bacterial receptors, preventing efficient phage binding, thereby reducing the number of bacteria killed. It Is known that E. coli in general produce a thicker EPS layer (Serra & Hengge, 2021) and that P. fluorescens produces less (Xu et al., 2024). This may be causing a higher cell lysis of P. fluorescens because due to a better diffusion of the phage in the presence of lower amounts of EPS.

The type of substrate appears to play a crucial yet indirect role in modulating bacterial inhibition. Although polystyrene and parchment paper exhibited similar phage release kinetics, the antimicrobial efficacy

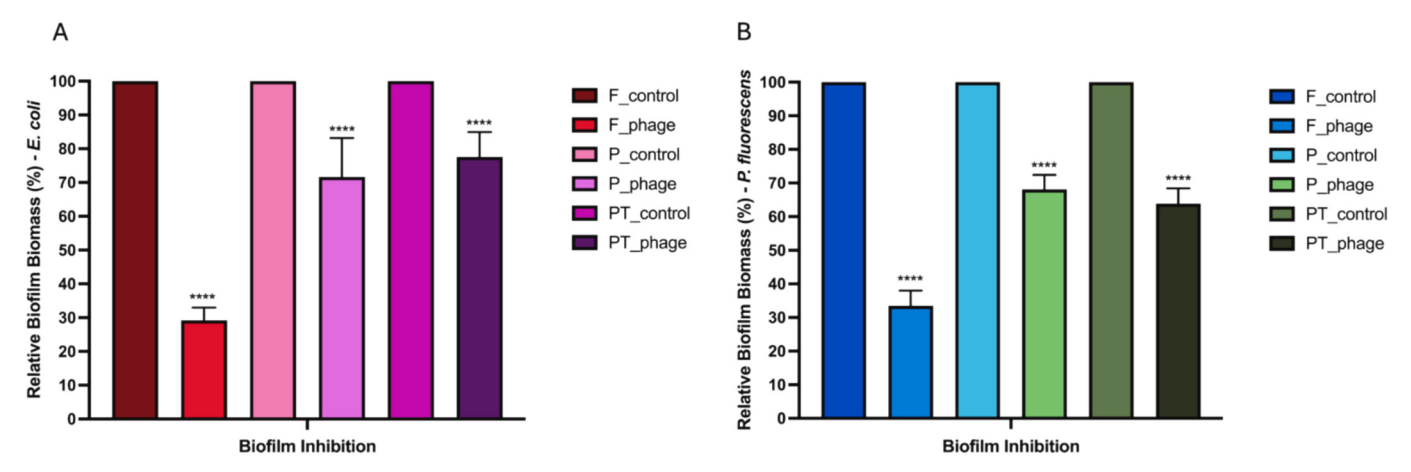


Fig. 4. Assessment of biofilm biomass using crystal violet staining. The graphs illustrate the inhibition of *E. coli* (A) and *P. fluorescens* (B) biofilms on different materials. F_control: Film without phages; F_phage: Film with phage cocktail; P_control: Parchment paper without phages; P_phage: Parchment paper with phage cocktail; PT_control: Polystyrene without phage cocktail; PT_phage: Polystyrene with phage cocktail. Data are presented as mean with error bars indicating standard deviation. (For interpretation of the references to colour in this figure legend, the reader is referred to the web version of this article.)

of phages incorporated into the polystyrene-based coating was lower for both P. fluorescens and E. coli. This difference cannot be solely attributed to direct bacterial adhesion to the substrate, since the inoculum was applied on the alginate layer. Rather, it likely arises from substrateinduced modifications in the physicochemical characteristics of the alginate coating itself. The substrate's hydrophobicity, surface energy, and microtopography can influence the film's interfacial morphology, porosity, and wettability, which in turn affect nutrient and moisture diffusion, and consequently bacterial colonization patterns on the coating surface (Costa et al., 2023; Kumar et al., 2019). In this context, the hydrophobic nature of polystyrene may have promoted stronger bacterial adhesion and the development of denser, more resistant biofilms on the coating surface, reducing phage accessibility and thus limiting antibacterial efficacy. Supporting this hypothesis, Wiguna et al. (2022) demonstrated that E. coli (enterohemorrhagic, enteropathogenic, and enterotoxigenic) and Bacillus cereus formed more persistent biofilms on polystyrene compared with stainless steel. Although their study did not include P. fluorescens, the observed trends for E. coli corroborate our findings, emphasizing that substrate-related properties can indirectly determine biofilm resilience and modulate the antimicrobial performance of phage-containing coatings.

3.3.2. Assessment of biofilm biomass by crystal violet

The CV biofilm quantification method revealed that the phages inhibited biofilm formation compared to the control (Fig. 4).

For E. coli, the most significant biofilm reduction after 24 h was observed in films, with a 70.8 % decrease in biofilm mass compared to the control, followed by parchment paper (28.4 %) and polystyrene (22.4 %). The results from both the CV staining and CFU analysis reveal interesting trends in the effectiveness of phage-incorporated films and coatings, depending on the material used. Both parchment paper and films resulted in similar viable cells numbers present after 24 h, however the CV staining results differ. One possible explanation for the discrepancy between the CV staining and CFU analysis could be related to the presence of dead cells and the efficiency of cell removal. Since CV stains both live and dead cells, a higher CV staining on parchment paper, despite similar viable cell numbers in the CFU analysis, may indicate a higher proportion of dead cells remaining attached to the biofilm matrix (Castro et al., 2022). Additionally, the difference in material properties might affect the removal of dead cells, with films potentially promoting more effective cell detachment and biofilm disruption, leading to a lower CV staining compared to parchment paper. This highlights how material properties influence not only phage activity but also the dynamics of biofilm formation and eradication.

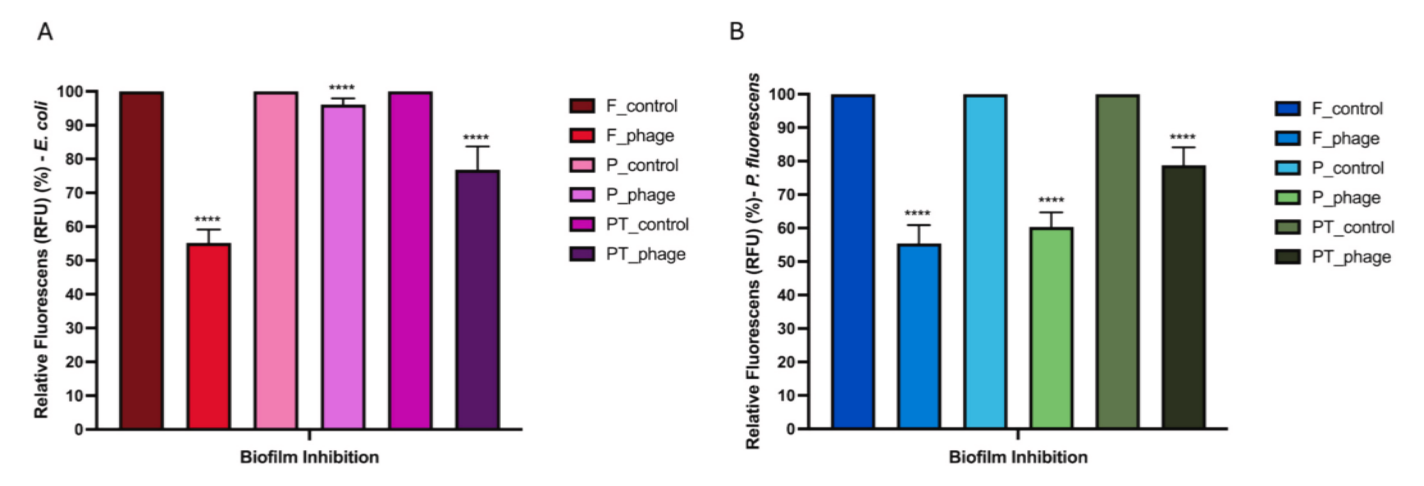


Fig. 5. Assessment of the metabolic activity of biofilms cells using the resazurin assay. The graphs show the inhibition of metabolic activity in *E. coli* (A) and *P. fluorescens* (B) biofilms on different materials. F_control: Film without phages; F_phage: Film with phage cocktail; P_control: Parchment paper without phages; P_phage: Parchment paper with phage cocktail; PT_control: Polystyrene without phage cocktail; PT_phage: Polystyrene with phage cocktail. Data are presented as mean with error bars indicating standard deviation.

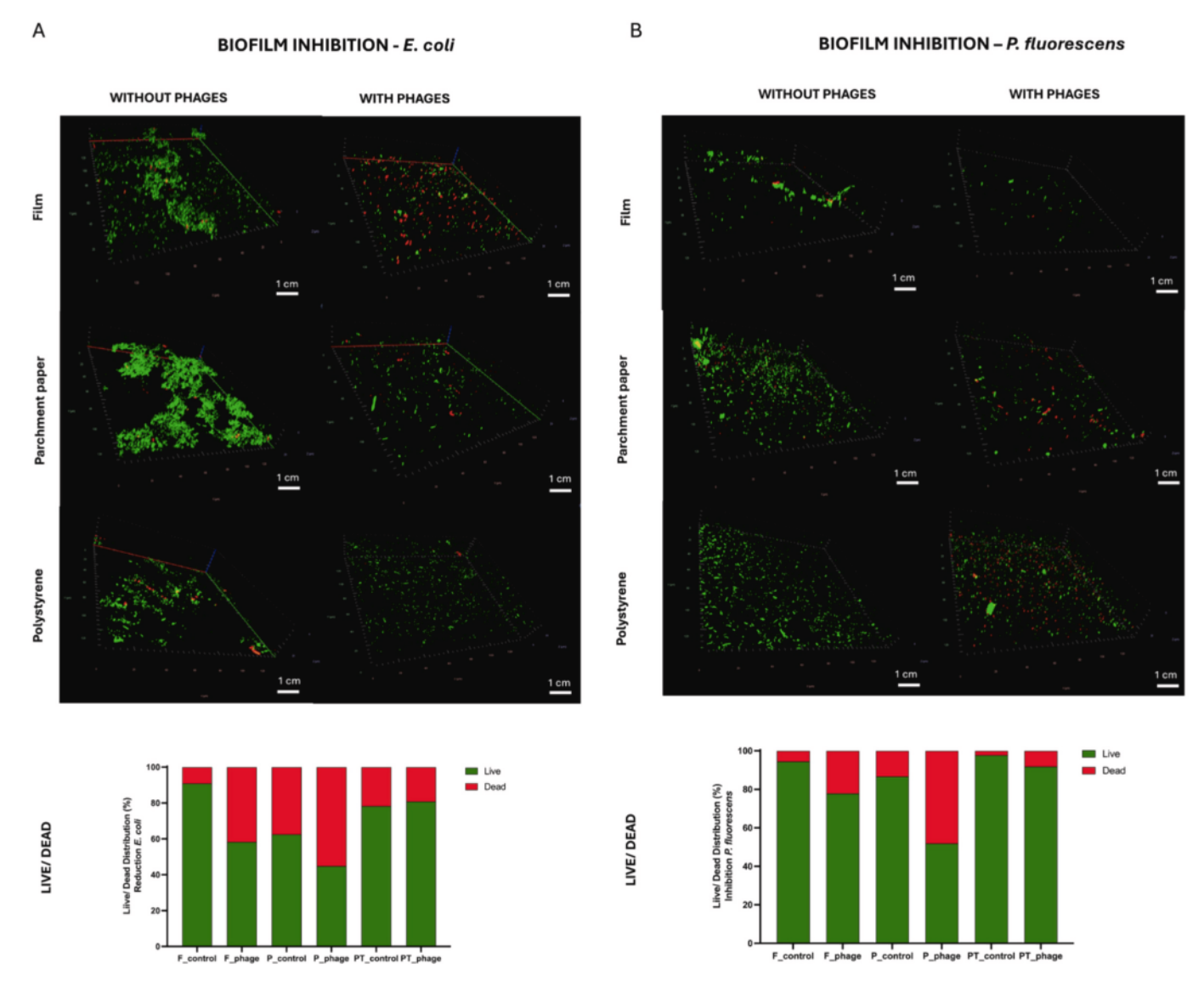


Fig. 6. Effect of phage treatment on bacterial biofilm inhibition in *E. coli* and *P. fluorescens* on different materials. F_control: Film without phages; F_phage: Film with phage cocktail; P_control: Parchment paper without phages; P_phage: Parchment paper with phage cocktail; PT_control: Polystyrene without phage cocktail; PT_phage: Polystyrene with phage cocktail. (A) Inhibition of biofilm formation after 24 h in *E. coli*. (B) Inhibition of biofilm formation after 24 h in *P. fluorescens*. Representative 3D images of biofilms were obtained via confocal laser scanning microscopy (CLSM), with live bacteria shown in green and dead bacteria in red. Scale bars in 3D-CLSM images are 1 cm. The graphs below show the quantitative analysis of live and dead bacterial cells, highlighting the effectiveness of phage-based films and coatings in controlling *E. coli* and *P. fluorescens* biofilms. (For interpretation of the references to colour in this figure legend, the reader is referred to the web version of this article.)

For *P. fluorescens*, the trend was somewhat similar but with varying reductions across the materials. After 24 h, films exhibited the highest inhibition (66.62 %), followed by polystyrene (36.17 %) and parchment paper (31.90 %). For *P. fluorescens*, the most substantial CFU reduction was observed in films, with a reduction of 2.72 logs compared to the untreated control, followed by parchment paper with a 2.56 log reduction compared to the untreated control.

3.3.3. Assessment of metabolic activity of biofilm cells by resazurin

The data obtained from the resazurin colorimetric assay demonstrated a reduction in the metabolic activity of all the groups tested with phages, to varying extents, when compared to the control group (Fig. 5). The results further support the trends observed in CFU counts and biofilm biomass reduction, reinforcing the influence of material type on phage efficacy.

For E. coli, films incorporated with phages exhibited the highest reduction in metabolic activity (44.81 %), followed by polystyrene

(23.16 %). Surprisingly, parchment paper presented only a 4 % difference in metabolic activity compared to the control, which shows that cells remain metabolically very active. For *P. fluorescens*, metabolic activity reductions reached a 44.56 % decrease in films, 39.67 %, in parchment paper and 21.19 % in polystyrene.

These findings align with CFU reduction data, where films also demonstrated higher reductions in bacterial counts, suggesting that this material may provide a more effective and sustained release of phages, leading to prolonged inhibition of metabolic activity. However, the discrepancy between metabolic activity and biomass reduction indicates that even though viable bacterial cells were still present, their metabolic state may have been altered, potentially due to stress induced by the phages.

3.3.4. Assessment of biofilm thickness and live/dead bacterial ratio using confocal microscopy and COMSTAT analysis

To evaluate the effectiveness of the coatings and films against E. coli

Table 1Different biofilm parameters analyzed during the inhibition *E. coli* using COM-STAT 2.1 software.

Bacteria	Matrix	Total biomass (µm³/ µm²)	Maximum thickness (μm)	Average thickness (biomass) (µm)	Surface to biovolume ratio (µm²/ µm³)
E. coli	F_control	$\begin{array}{c} 3.40 \pm \\ 0.55 \end{array}$	9.00 ± 0.76 ^A	$2.75 \pm 0.32 ^{\text{A}}$	$8.06 \pm \\ 0.34 ^{\text{A}}$
	F_phage	2.56 ± 0.37^{B}	4.54 ± 0.98 ^B	1.68 ± 0.45^{B}	6.49 ± 0.53 ^B
	P_control	$\begin{array}{c} 4.72 \pm \\ 0.43^{C} \end{array}$	$18.00 \pm \\ 0.63^{\mathrm{C}}$	8.82 ± 0.52^{C}	$7.68 \pm 0.$ 66^{C}
	P_phage	$\begin{array}{c} 1.04 \pm \\ 0.06^{\mathrm{D}} \end{array}$	$\begin{array}{c} 5.00 \; \pm \\ 1.3^{\text{B}} \end{array}$	$\begin{array}{c} 2.66 \; \pm \\ 0.32^{\mathrm{D}} \end{array}$	$5.21 \pm 0.$ 28^{D}
	PT_control	$\begin{array}{c} 6.59 \pm \\ 0.62^E \end{array}$	$18.00 \pm \\1.76^{\rm C}$	$14.22 \pm \\ 0.27^{\mathrm{E}}$	$4.53 \pm 0.$ 33^{E}
	PT_phage	$\begin{array}{c} 5.31 \pm \\ 0.21^F \end{array}$	$17.00\ \pm$ 1.25^{D}	$\begin{array}{l} \textbf{3.16} \pm \\ \textbf{0.42}^{\text{F}} \end{array}$	$\begin{array}{l} 3.31 \pm \\ 0.53^F \end{array}$
P. fluorescens	F_control	$\begin{array}{c} 1.97 \; \pm \\ 0.02^{\text{A}} \end{array}$	$\begin{array}{c} 3.00 \; \pm \\ 0.45 \; ^{\rm A} \end{array}$	$\begin{array}{c} 2.06 \pm \\ 0.74^{\text{A}} \end{array}$	$5.76~\pm$ $0.03~^{\rm A}$
	F_phage	$\begin{array}{c} 0.80 \; \pm \\ 0.00^B \end{array}$	$\begin{array}{c} 1.00 \pm \\ 0.02^{\mathrm{B}} \end{array}$	$\begin{array}{c} 1.00\ \pm \\ 0.04^{B} \end{array}$	$\begin{array}{c} 3.33 \pm \\ 0.20^{B} \end{array}$
	P_control	$\begin{array}{c} 4.80 \pm \\ 0.43^{C} \end{array}$	$7.00 \pm 0.34^{\rm C}$	7.79 ± 0.87^{C}	$\begin{array}{c} \textbf{4.90} \pm \\ \textbf{0.15}^{\text{C}} \end{array}$
	P_phage	$\begin{array}{c} 4.10 \pm \\ 0.32^D \end{array}$	$\begin{array}{c} 5.00 \pm \\ 0.54^{\mathrm{D}} \end{array}$	$\begin{array}{c} 2.08 \pm \\ 0.20^{A} \end{array}$	$\begin{array}{c} \textbf{4.07} \pm \\ \textbf{0.12}^{\text{D}} \end{array}$
	PT_control	$\begin{array}{c} 5.90 \; \pm \\ 0.21^E \end{array}$	$\begin{array}{c} 20.00 \; \pm \\ 1.02^E \end{array}$	$\begin{array}{c} \textbf{7.06} \pm \\ \textbf{0.09}^{\text{CD}} \end{array}$	$\begin{array}{c} 7.15\pm0.\\ 35^E \end{array}$
	PT_phage	$\begin{array}{c} 5.10 \pm \\ 0.65^{\mathrm{F}} \end{array}$	$16.00 \pm \\1.22^F$	$\begin{array}{c} \textbf{6.83} \pm \\ \textbf{0.11}^{\text{D}} \end{array}$	$\begin{array}{c} 5.26\pm0.\\ 23^F \end{array}$

Superscript letters (A-F): Within each respective material group, values in the same column not sharing upper case superscript letters indicate statistically significant differences between each other (p < 0.05).

and *P. fluorescens*, confocal laser scanning microscopy (CLSM) was employed after staining the bacteria to assess their viability (Fig. 6).

In the *E. coli* inhibition experiments, the 3D confocal images revealed a promising performance in the groups treated with phage-infused films and phage-coated parchment paper. These findings were further corroborated by quantitative Live/Dead analysis, demonstrating a reduction in live cells of 18.65 % for F_phage-treated samples, 17.11 % for P_phage-treated samples. The F_control samples were strongly viable, PT_control had mostly viable cells while the P_control had already a high number of dead cells. The live/dead results obtained with PT_control were comparable to the phage treated samples. This may indicate that the biofilm formed is either stronger of that the phages may be non-specifically binding to the substrate and thus not interact with

the bacteria.

In the *P. fluorescens*, inhibition experiments a similar trend was observed, where the 3D confocal images also demonstrate the efficacy of phage-infused films and phage-coated parchment paper samples in reducing biofilm formation. These observations were confirmed by quantitative Live/Dead analysis, which revealed a reduction in live cells of 22.15 % for F_phage-treated samples, 48.10 % for P_phage-treated samples, and 8.15 % for PT_phage-treated samples. Furthermore, all control samples are strongly viable compared to the *E. coli* experiment, even the P_control samples (~87 %). The higher viability of *P. fluorescens* is likely to be related with its motility characteristics which aid the bacteria to have better access to nutrients and oxygen (Zegadlo et al., 2023; Kumar et al., 2019), while *E. coli* may be having oxygen and nutrient limitations due to the formation of clusters and thus a higher number of dead cells in these regions (Amato & Brynildsen, 2014; Rooney et al., 2020).

COMSTAT analysis was performed to quantitatively assess biofilm structural parameters and compare differences between experimental conditions. This approach enables a detailed evaluation of biofilm architecture, providing insights into variations in biomass distribution, thickness, roughness, and surface-to-volume ratio.

The quantitative analysis (COMSTAT) of the 3D images obtained for the inhibition of *E. coli* biofilm (Table 1) revealed that all parameters analyzed (total biomass, maximum thickness, average thickness [biomass], and surface-to-biovolume ratio) showed significant differences between the phage-treated groups and the control group.

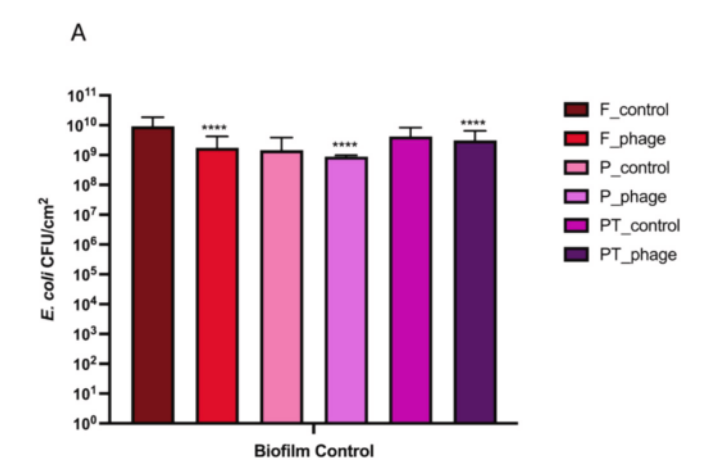
In contrast, the quantitative analysis of the average thickness (biomass) parameter for P. fluorescens inhibition (Table 1) revealed no significant difference between PT_control and PT_phage. This finding aligns with the Live/Dead assay data, which showed only a 8.15 % reduction in live cells for PTC-treated samples.

Polystyrene is commonly used for packaging meat and fruits due to its durability, low cost, and ease of production, making it a widely utilized material in the food industry. Our findings align with the study by Wiguna et al. (2022), which demonstrated that polystyrene surfaces exhibited stronger biofilm formation compared to stainless steel. Surface properties significantly influence bacterial adhesion, and biofilms formed on polystyrene are more robust and resistant to removal than those formed on stainless steel.

3.4. Biofilm control experiments

3.4.1. Assessment of biofilm viable cells by colony count

Eliminating mature biofilms from surfaces is more challenging than preventing their formation, as the extracellular polymeric substances



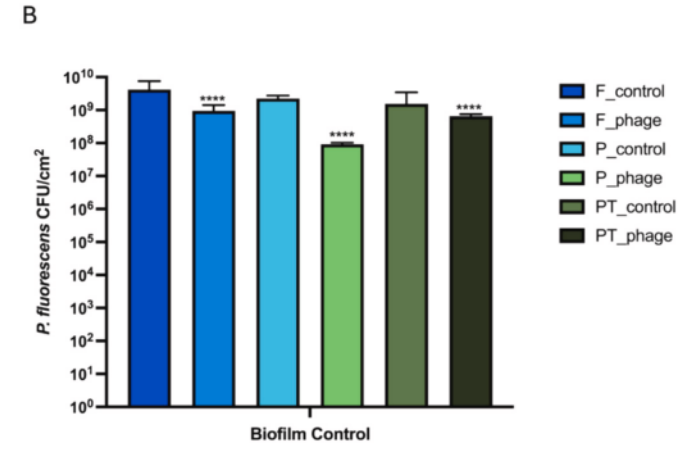


Fig. 7. Viable cell counts (CFU/mL) of *E. coli* (A) and *P. fluorescens* (B) after 48-h assays on different materials. F_control: Film without phages; F_phage: Film with phage cocktail; P_control: Parchment paper without phages; P_phage: Parchment paper with phage cocktail; PT_control: Polystyrene without phage cocktail; PT_phage: Polystyrene with phage cocktail. Bars represent the mean CFU/mL with error bars indicating standard deviation. ****: *P* < 0.0001.

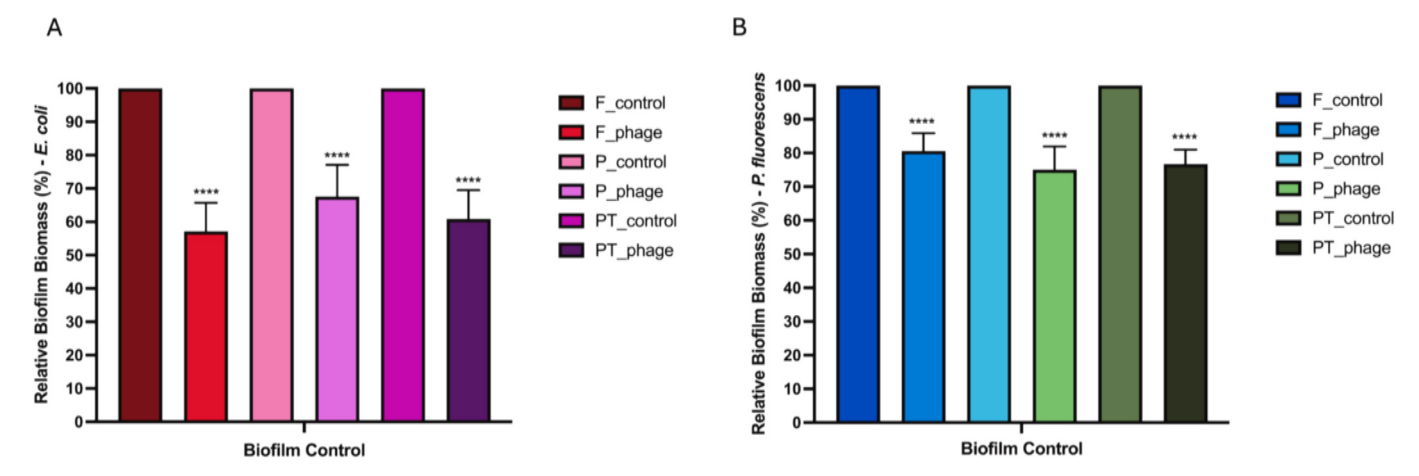


Fig. 8. Assessment of biofilm biomass using crystal violet staining. The graphs illustrate the biofilm control of *E. coli* (A) and *P. fluorescens* (B) on different materials. F_control: Film without phages; F_phage: Film with phage cocktail; P_control: Parchment paper without phages; P_phage: Parchment paper with phage cocktail; PT_control: Polystyrene without phage cocktail; PT_phage: Polystyrene with phage cocktail. Data are presented as mean with error bars indicating standard deviation. (For interpretation of the references to colour in this figure legend, the reader is referred to the web version of this article.)

(EPS) in biofilms shield bacteria from inactivation or removal under stress conditions (Shen et al., 2021). Therefore, beyond biofilm prevention, this study systematically assessed the eradication of preestablished biofilms (24 h) that were treated for 24 h using a phage cocktail incorporated into films or substrate coatings. Given the protective nature of biofilms, evaluating the same multiple parameters as in 3.3 was essential to gaining a comprehensive understanding of the phages' antimicrobial action.

Control experiments showed that for *E. coli*, the greatest reduction in CFU occurred on phage-loaded films, with a 0.72 log decrease, followed by parchment paper with a 0.21 log reduction, and polystyrene with a 0.13 log decrease compared to the control (Fig. 7). In contrast, for *P. fluorescens*, the highest inhibition was observed on phage-loaded parchment paper, resulting in a 1.39 log reduction, followed by films with a 0.65 log decrease, and polystyrene with a 0.38 log reduction. CFU/mL values for *E. coli* and *P. fluorescens* during the 48-h evaluation deviated from the previously observed trends (inhibition studies). In general, inhibition studies for both *E. coli* and *P. fluorescens* phage-treated samples a higher reduction of viable cells, particularly in the case of films and parchment paper.

The lower efficacy observed against pre-formed biofilms is consistent with the complex nature of phage–biofilm interactions. Several studies

have demonstrated that the extracellular polymeric substances (EPS) matrix can act as a diffusion barrier, limiting phage penetration and reducing their ability to reach and lyse embedded bacterial cells. Moreover, components of the EPS, such as polysaccharides and proteins, may inactivate or sequester phages, further reducing their effectiveness. In addition, the physiological heterogeneity of bacterial populations within biofilms plays a critical role: cells in different metabolic states (e. g., stationary-phase cells) can exhibit lower susceptibility to phage infection compared to actively dividing cells (Melo et al., 2018; Pires et al., 2021). Taken together, these factors provide a plausible explanation for the reduced antimicrobial performance observed in our study when phages were applied against mature biofilms.

3.4.2. Assessment of biofilm biomass by crystal violet

The CV biofilm quantification method revealed that biofilm formation was reduced under the tested conditions with phages compared to the control, Fig. 8.

After 48 h, biofilm reduction in *E. coli* remained evident across all materials, though to a lesser extent. Films exhibited the highest reduction (42.88 %), followed by polystyrene (39.20 %) and parchment paper (32.45 %). For *P. fluorescens*, biofilm reduction was lower across all materials, with films showing a 19.44 % reduction, parchment paper

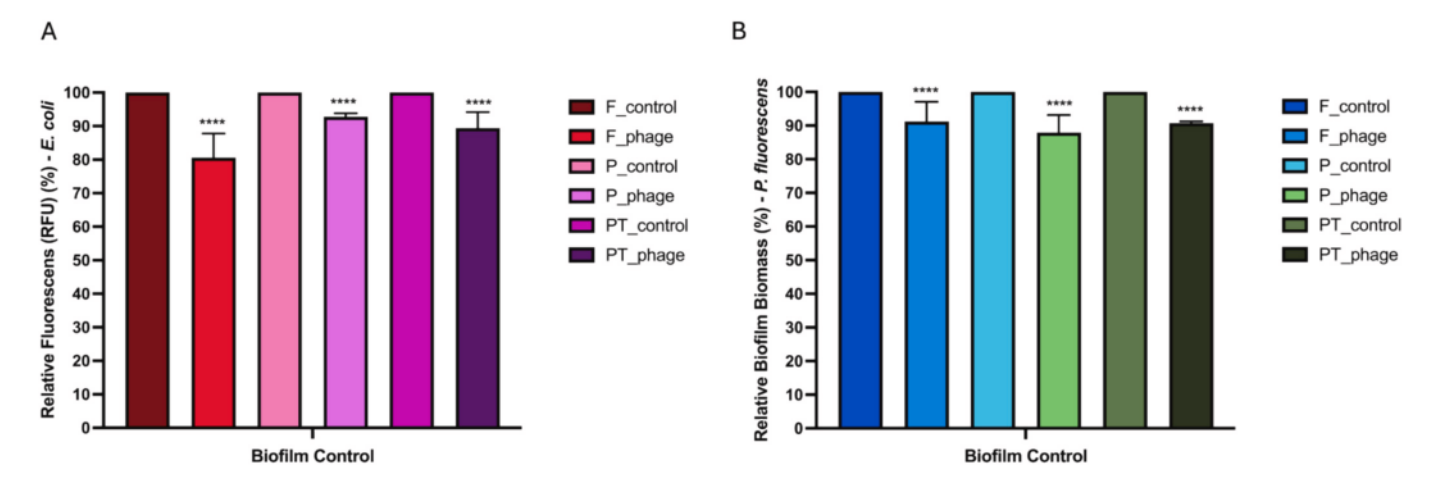


Fig. 9. Assessment of the metabolic activity of biofilms cells using the resazurin assay. The graphs show the inhibition and reduction of metabolic activity in *E. coli* (A) and *P. fluorescens* (B) biofilms on different materials. F_control: Film without phages; F_phage: Film with phage cocktail; P_control: Parchment paper without phages; P_phage: Parchment paper with phage cocktail; PT_control: Polystyrene without phage cocktail; PT_phage: Polystyrene with phage cocktail. Data are presented as mean with error bars indicating standard deviation.

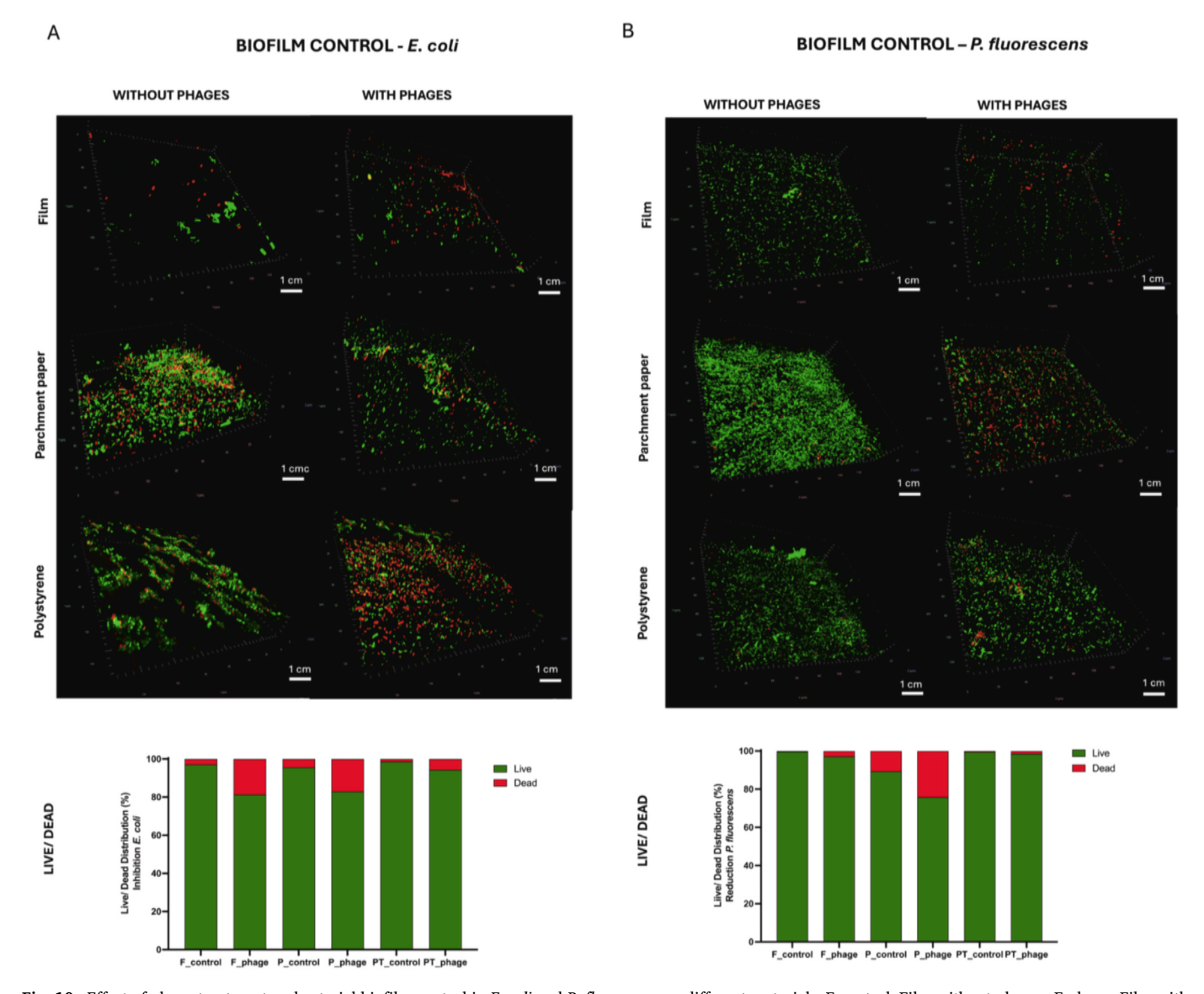


Fig. 10. Effect of phage treatment on bacterial biofilm control in *E. coli* and *P. fluorescens* on different materials. F_control: Film without phages; F_phage: Film with phage cocktail; P_control: Parchment paper without phages; P_phage: Parchment paper with phage cocktail; PT_control: Polystyrene without phage cocktail; PT_phage: Polystyrene with phage cocktail. (A) Control of mature biofilms after 48 h of treatment in *E. coli*. (B) Control of mature biofilms after 48 h of treatment in *P. fluorescens*. Representative 3D images of biofilms were obtained via confocal laser scanning microscopy (CLSM), with live bacteria shown in green and dead bacteria in red. Scale bars in 3D-CLSM images are 1 cm. The graphs below show the quantitative analysis of live and dead bacterial cells, highlighting the effectiveness of phage-based films and coatings in controlling *E. coli* biofilms. (For interpretation of the references to colour in this figure legend, the reader is referred to the web version of this article.)

24.98 %, and polystyrene 23.28 %. The overall reduction was significantly smaller compared to $E.\ coli$, possibly due to differences in biofilm structure or bacterial response to phage treatment.

CV values after 48 h deviated from expected trends (inhibition experiments). Overall, there was a significant difference in biofilm biomass in both experiments, with a lower reduction of biomass in the assays performed on 24 h pre-formed biofilms. This decline in antimicrobial efficacy in the control experiments may be due to the film or coating matrix limiting phage access to bacterial cells located in deeper biofilm layers. Additionally, as described above, the metabolic state of bacteria may play a role in phage effectiveness.

3.4.3. Assessment of metabolic activity of biofilm cells by resazurin

The data obtained from the resazurin colorimetric assay demonstrated a reduction in the metabolic activity of all the groups tested with phages, to varying extents, when compared to the control group (Fig. 9).

The metabolic activity results for biofilm inhibition contrast with the

biomass reduction observed in the biofilm control. For *E. coli*, metabolic activity decreased by 19.44 % in films, 7.22 % on parchment paper, and 10.57 % on polystyrene. For *P. fluorescens*, the reductions were 8.76 % in films, 12.09 % on parchment paper, and 9.25 % on polystyrene. These findings suggest that while the biofilm structure was somewhat disrupted, a portion of the bacterial population remained metabolically active. The variations across different materials further highlight the influence of the matrix on phage-bacteria interactions. These findings underscore the complexity of phage-based antimicrobial strategies and the need for optimized material formulations to enhance phage release and long-term effectiveness.

3.4.4. Assessment of biofilm thickness and live/dead bacterial ratio using confocal microscopy and COMSTAT analysis

To evaluate the effectiveness of the active packaging against $E.\ coli$ and $P.\ fluorescens$ biofilms, CLSM was employed to assess bacterial viability (Fig. 10).

Table 2Different biofilm parameters analyzed during the reduction *E. coli* using COM-STAT 2.1 software.

Bacteria	Matrix	Total biomass (μm ³ / μm ²)	Maximum thickness (μm)	Average thickness (biomass) (µm)	Surface to biovolume ratio (µm²/ µm³)
E. coli	F_control	$\begin{array}{c} 2.71\ \pm \\ 0.32\ ^{\rm A} \end{array}$	$7\pm0.89~^{A}$	$2.66 \pm \\ 0.65 ^{\text{A}}$	$7.96 \pm \\ 0.23 ^{\text{A}}$
	F_phage	1.5 ± 0.43 ^B	2 ± 0.35^B	$1.02 \pm 0.08^{\mathrm{B}}$	6.53 ± 0.18^{B}
	P_control	8.0 ± 0.28 ^C	$\begin{array}{c} 26 \pm \\ 1.67^{\mathrm{C}} \end{array}$	12.06 ± 0.12^{C}	9.47 ± 0.31 ^C
	P_phage	4.04 ± 0.63 ^D	10 ± 0.86 ^D	8.12 ± 0.15^{D}	4.97 ± 0.27^{D}
	PT_control	$\begin{array}{c} 3.73 \pm \\ 0.21^E \end{array}$	$\begin{array}{c} 24 \pm \\ 1.93^{\rm E} \end{array}$	$\begin{array}{c} 10 \pm \\ 0.17^{\rm E} \end{array}$	$\begin{array}{c} 8.72 \pm \\ 0.25^E \end{array}$
	PT_phage	$\begin{array}{c} 2.27 \pm \\ 0.11^F \end{array}$	8 ± 0.92^F	$\begin{array}{c} 8.77 \pm \\ 0.02^F \end{array}$	$\begin{array}{c} 5.53 \pm \\ 0.12^{F} \end{array}$
P. fluorescens	F_control	$^{\rm 4.6~\pm}_{\rm 0.15~^{\rm A}}$	8 \pm 0.63 $^{\text{A}}$	$10.28~\pm\\0.12~^{\rm A}$	$\begin{array}{c} 5.31 \; \pm \\ 0.35 \; ^{\rm A} \end{array}$
	F_phage	$\begin{array}{c} 2.1 \; \pm \\ 0.04^{B} \end{array}$	4 ± 0.82^B	$\begin{array}{c} 1.01 \; \pm \\ 0.03^{\mathrm{B}} \end{array}$	$\begin{array}{c} \textbf{4.30} \pm \\ \textbf{0.27}^{\text{B}} \end{array}$
	P_control	$\begin{array}{c} 8.88 \pm \\ 0.29^{\mathrm{C}} \end{array}$	$\begin{array}{c} 31 \pm \\ 0.61^{\rm C} \end{array}$	$24.61 \pm \\2.88^{\mathrm{C}}$	$31.35 \pm \\1.45^{\rm C}$
	P_phage	$\begin{array}{c} 6.88 \pm \\ 0.11^{\mathrm{D}} \end{array}$	7 ± 0.89^D	$11.19~\pm\\0.98^{\mathrm{D}}$	$\begin{array}{c} 5.84 \pm \\ 0.31^{\mathrm{D}} \end{array}$
	PT_control	$\begin{array}{l} 5.5 \pm \\ 0.21^E \end{array}$	8 ± 0.76 A	$\begin{array}{c} 12.09 \; \pm \\ 0. \; 21^D \end{array}$	$\begin{array}{c} 8.16 \pm \\ 0.23^E \end{array}$
	PT_phage	$\begin{array}{c} 4.3 \pm \\ 0.17^{F} \end{array}$	7 ± 0.35^{D}	$\begin{array}{c} 10 \pm \\ 0.11^E \end{array}$	$\begin{array}{c} \textbf{5.77} \pm \\ \textbf{0.13}^{\text{F}} \end{array}$

Superscript letters (A-F): Within each respective material group, values in the same column not sharing upper case superscript letters indicate statistically significant differences between each other (p < 0.05).

Table 3Antibacterial efficacy of various material matrices against FSB24 and North phages after 24 h.

Matrix (Cheese)		Antibacterial activity (A) 24 h	Efficacy of antibacterial property
FSB24	Parchment Paper	2.49	Significant
phages	Polystyrene substrates	1.47	Low
	Film	2.35	Significant
North	Parchment Paper	2.25	Significant
phages	Polystyrene substrates	1.73	Low
	Film	2.36	Significant

When assessing biofilm eradication for *E. coli*, the 3D confocal images indicated greater resistance to biofilm removal. Nonetheless, the quantitative Live/Dead ratio analysis showed a reduction in live cells of 41.70 % for phage-infused films, 55.15 % for phage-coated parchment paper, and 19.14 % for PT_phage-treated samples.

In the biofilm eradication experiments for *P. fluorescens*, however, the 3D confocal images showed greater resistance to biofilm removal compared to the inhibition experiments. This was reflected in the quantitative Live/Dead analysis, which indicated a reduction in live cells of only 2.88 % for phage-infused films, 24.16 % for phage-coated parchment paper, and 1.47 % for PT_phage-treated samples

Quantitative analysis (COMSTAT) of the 3D images obtained for the *E. coli* and *P. fluorescens* (Table 2) biofilm controls revealed significant differences in all analyzed parameters—total biomass, maximum thickness, average thickness (biomass), and surface-to-biovolume ratio—between phage-treated groups and the control. These findings indicate that while biofilm eradication was less pronounced, phage

Table 4Antibacterial efficacy of various material matrices against FSB24 and North phages after 7 days.

Matrix (Cheese)		Antibacterial activity (A) 7 days	Efficacy of antibacterial property
FSB24	Parchment Paper	1.91	Low
phages	Polystyrene substrates	0.35	Low
	Film	0.83	Low
North	Parchment Paper	1.33	Low
phages	Polystyrene substrates	0.26	Low
	Film	1.27	Low

treatment still led to measurable reductions compared to untreated samples.

3.5. Antimicrobial activity of bacteriophage-loaded sodium alginatebased films and coatings in cheese samples

The antibacterial activity of the samples was evaluated according to the ISO 22196 standard in cheese samples. As per this standard, antibacterial activity (A) is classified as follows: A < 2 indicates low antibacterial efficacy, $2 \leq A < 3$ indicates significant efficacy, and $A \geq 3$ indicates strong antibacterial efficacy.

The results summarized in Table 3 reveal significant variability in the antibacterial efficacy of phage-based treatments depending on the material matrix, bacterial strain, and time. At the 24-h mark, phage-coated parchment paper and phage-infused films demonstrated significant antibacterial ($2 \le A < 3$) activity against both *P. fluorescens* and *E. coli*. Parchment paper exhibited antibacterial activity values of 2.49 and 2.25 for P. fluorescens and E. coli, respectively, indicating its effectiveness as a short-term phage delivery system. Similarly, films achieved significant activity values of 2.35 for P. fluorescens and 2.36 for E. coli, showcasing their efficiency as a delivery matrix. On the other hand, polystyrene substrates exhibited only low antimicrobial activity (A < 2), suggesting that this matrix is less effective in facilitating phage-biofilm interactions compared to parchment paper and films. After 7 days, a noticeable decline in antibacterial efficacy was observed (Table 4). The antibacterial activity of parchment paper decreased from significant at 24 h to low at 7 days. Polystyrene substrates, which initially showed low efficacy (1.47), maintained this trend but also, the value observed reduced from 24 h to 7 days. The results of the antibacterial activity tests align with the biofilm inhibition and eradication data presented in Figs. 6 and 10.

Although sensory properties such as texture, flavor, and overall acceptance were not evaluated in this study, literature suggests that sodium alginate coatings generally have minimal impact on taste and may improve visual and textural attributes of cheeses (e.g., improved softness, gloss, reduced weight loss) (Kampf & Nussinovitch, 2000; Xue et al., 2025; Pieretti et al., 2019).

Overall, these findings emphasize the critical role of material properties in determining the success of phage-based antibacterial interventions. Parchment paper and films emerged as the most effective delivery systems, particularly against *E. coli*, while polystyrene substrates exhibited limited antibacterial performance. Moreover, the data underscore the necessity of tailored approaches to target resilient biofilms, such as those formed by *P. fluorescens*.

4. Conclusion

The present study demonstrated that incorporation of bacteriophages into alginate-based films and coatings for paper and plastic substrates effectively inhibited and reduced biofilms of *E. coli* and *P. fluorescens*, as confirmed through viable cell counts, biomass quantification, metabolic activity measurements, and live/dead staining. Application of these phage-loaded materials to cheese samples over a 7-day period further showed that antibacterial efficacy is influenced by the type of material matrix, bacterial strain, and duration of exposure. While phage release from coatings was similar across substrates, differences in coating-substrate interactions and surface topography may also affect biofilm control, highlighting an important aspect for future investigation. These findings underscore the potential of phage-infused alginate materials as antimicrobial strategies in food-related applications and emphasize the need for further optimization of phage formulations, complementary antimicrobials, and material surface properties to achieve sustained and effective biofilm management.

CRediT authorship contribution statement

Fernanda Coelho: Writing – review & editing, Writing – original draft, Methodology, Investigation, Funding acquisition, Formal analysis, Data curation, Conceptualization. Larissa Ribas Fonseca: Investigation. Lorenzo Pastrana: Supervision, Funding acquisition. Sanna Sillankorva: Writing – review & editing, Writing – original draft, Supervision, Methodology, Funding acquisition, Conceptualization. Valtencir Zucolotto: Writing – review & editing, Supervision, Funding acquisition.

Funding sources

The authors acknowledge final supported from the FAPESP (Grant No. 2023/14222-7).

Declaration of competing interest

The authors declare the following financial interests/personal relationships which may be considered as potential competing interests: Fernanda Coelho reports financial support was provided by State of Sao Paulo Research Foundation. If there are other authors, they declare that they have no known competing financial interests or personal relationships that could have appeared to influence the work reported in this paper.

Acknowledgements

Sanna Sillankorva acknowledges funding by FCT through the individual scientific employment program contract (2020.03171.CEECIND).

Appendix A. Supplementary data

Supplementary data to this article can be found online at https://doi.org/10.1016/j.foodres.2025.117859.

Data availability

Data will be made available on request.

References

- Alves, D., Marques, A., Milho, C., Costa, M. J., Pastrana, L. M., Cerqueira, M. A., & Sillankorva, S. M. (2019). Bacteriophage φIBB-PF7A loaded on sodium alginate-based films to prevent microbial meat spoilage. *International Journal of Food Microbiology*, 291, 121–127. https://doi.org/10.1016/j.iifoodmicro.2018.11.026
- Amato, S. M., & Brynildsen, M. P. (2014). Nutrient transitions are a source of Persisters in Escherichia coli biofilms. *PLoS One*, 9(3), Article e93110. https://doi.org/10.1371/journal.pone.0093110
- Berti, S., & Oll´e Resa, C. P., Basanta, F., Gerschenson, L.N., Jagus, R.J.. (2019). Edible coatings on gouda cheese as a barrier against external contamination during ripening. Food Bioscience, 31(100447), 2019. https://doi.org/10.1016/j.fbio.2019.100447
- Bremer, B., & Seale, B. (2009). Biofilms in dairy processing. In P. M. Fratamico, B. A. Annous, & N. W. Gunther (Eds.), *Biofilms in the food and beverage industries* (pp. 396–431). Boca Raton: CRC Press.

- Castro, J., Lima, Â., Sousa, L. G. V., Rosca, A. S., Muzny, C. A., & Cerca, N. (2022). Crystal violet staining alone is not adequate to assess synergism or antagonism in multispecies biofilms of Bacteria associated with bacterial vaginosis. Frontiers in Cellular and Infection Microbiology, 11, Article 795797. https://doi.org/10.3389/fcimb.2021.795797
- Costa, M. J., Pastrana, L. M., Teixeira, J. A., Sillankorva, S. M., & Cerqueira, M. A. (2023). Bacteriophage delivery Systems for Food Applications: Opportunities and perspectives. Viruses, 15(6), 1271. https://doi.org/10.3390/v15061271
- Cui, H., Yuan, L., & Lin, L. (2017). Novel chitosan film embedded with liposomeencapsulated phage for biocontrol of Escherichia coli O157: H7 in beef. Carbohydrate Polymers, 177, 156–164.
- Dhulipalla, H., Basavegowda, N., Haldar, D., et al. (2025). Integrating phage biocontrol in food production: Industrial implications and regulatory overview. *Discov Appl Sci*, 7, 314. https://doi.org/10.1007/s42452-025-06754-3
- Eneroth, A., Ahrné, S., & Molin, G. (2000). Contamination of milk with gram-negative spoilage bacteria during filling of retail containers. *Int J Food Microb*, 10, 99–106.
- Figueiredo, C. M., Malvezzi Karwowski, M. S., da Silva Ramos, R. C. P., de Oliveira, N. S., Peña, L. C., Carneiro, E., & Rosa, E. A. R. (2021). Bacteriophages as tools for biofilm biocontrol in different fields. *Biofouling*, 37(6), 689–709. https://doi.org/10.1080/ 08927014.2021.1955866
- García-Anaya, M. C., Sepulveda, D. R., Zamudio-Flores, P. B., & Acosta-Muñiz, C. H. (2023). Bacteriophages as additives in edible films and coatings. *Trends in Food Science & Technology*, 132, 150–161. https://doi.org/10.1016/j.tifs.2023.02.015
- Gopal, N., Hill, C., Ross, P. R., Beresford, T. P., Fenelon, M. A., & Cotter, P. D. (2015). The prevalence and control of Bacillus and related spore-forming Bacteria in the dairy industry. Frontiers in Microbiology, 6, 1418. https://doi.org/10.3389/ fmicb.2015.01418
- Hammad, A. M., Eltahan, A., Hassan, H. A., Abbas, N. H., Hussien, H., & Shimamoto, T. (2022). Loads of coliforms and fecal coliforms and characterization of Thermotolerant Escherichia coli in fresh raw Milk cheese. Foods (Basel, Switzerland), 11(3), 332. https://doi.org/10.3390/foods11030332
- Han, A., & Lee, S. Y. (2023). An overview of various methods for in vitro biofilm formation: A review. Food Science and Biotechnology, 32(12), 1617–1629. https://doi. org/10.1007/s10068-023-01425-8
- Heydorn, A., Nielsen, A. T., Hentzer, M., Sternberg, C., Givskov, M., Ersbøll, B. K., & Molin, S. (2000). Quantification of biofilm structures by the novel computer program COMSTAT. *Microbiology (Reading, England)*, 146(Pt 10), 2395–2407. https://doi.org/10.1099/00221287-146-10-2395
- Kamdar, S., Ghosh, D., Lee, W., Tătulea-Codrean, M., Kim, Y., Ghosh, S., Kim, Y., Cheepuru, T., Lauga, E., Lim, S., & Cheng, X. (2023). Multiflagellarity leads to the size-independent swimming speed of peritrichous bacteria. Proceedings of the National Academy of Sciences of the United States of America, 120(48), Article e2310952120. https://doi.org/10.1073/pnas.2310952120
- Kampf, N., & Nussinovitch, A. (2000). Hydrocolloid coating of cheeses. Food Hydrocolloids, 14(6), 531–537.
- Kumar, H., Franzetti, L., Kaushal, A., et al. (2019). Pseudomonas fluorescens: A potential food spoiler and challenges and advances in its detection. Annales de Microbiologie, 69, 873–883. https://doi.org/10.1007/s13213-019-01501-7
- Melo, L. D. R., França, A., Brandão, A., Sillankorva, S., Cerca, N., & Azeredo, J. (2018). Assessment of Sep1virus interaction with stationary cultures by transcriptional and flow cytometry studies. FEMS Microbiology Ecology, 94(10). https://doi.org/ 10.1093/femsec/fiy143
- Milho, C., Silva, M. D., Sillankorva, S., & Harper, D. R. (2021). Biofilm applications of bacteriophages. In D. R. Harper, S. T. Abedon, B. H. Burrowes, & M. L. McConville (Eds.), Bacteriophages. Cham: Springer. https://doi.org/10.1007/978-3-319-41986-2 27.
- Papadochristopoulos, A., Kerry, J. P., Fegan, N., Burgess, C. M., & Duffy, G. (2021). Natural anti-Microbials for enhanced microbial safety and shelf-life of processed packaged meat. Foods (Basel, Switzerland), 10(7), 1598. https://doi.org/10.3390/foods10071598
- Pieretti, G, G., Pinheiro, M, P., Scapim, M,R,S., Mikcha, J,M,G; Madrona,G,S. (2019). Effect of an edible alginate coating with essential oil to improve the quality of a fresh cheese. Acta Scientiarum. Technology, State University of Maringá, 41. doi: https://doi.org/10.4025/actascitechnol.v41i1.36402.
- Pires, D. P., Melo, L. D. R., & Azeredo, J. (2021). Understanding the complex phage-host interactions in biofilm communities. *Annual Review of Virology*, 8(1), 73–94. https://doi.org/10.1146/annurev-virology-091919-074222
- Proulx, J., Sullivan, G., Marostegan, L. F., VanWees, S., Hsu, L. C., & Moraru, C. I. (2017).
 Pulsed light and antimicrobial combination treatments for surface decontamination of cheese: Favorable and antagonistic effects. *Journal of Dairy Science*, 100(3), 1664–1673. https://doi.org/10.3168/jds.2016-11582
- Radford, D., Guild, B., Strange, P., Ahmed, R., Lim, L. T., & Balamurugan, S. (2017). Characterization of antimicrobial properties of Salmonella phage Felix O1 and Listeria phage A511 embedded in xanthan coatings on poly(lactic acid) films. Food Microbiology, 66, 117–128. https://doi.org/10.1016/j.fm.2017.04.015
- Rooney, L. M., Amos, W. B., Hoskisson, P. A., & McConnell, G. (2020). Intra-colony channels in E. Coli function as a nutrient uptake system. *The ISME Journal*, 14(10), 2461–2473. https://doi.org/10.1038/s41396-020-0700-9
- Serra, D. O., & Hengge, R. (2021). Bacterial multicellularity: The biology of Escherichia coliBuilding large-scale biofilm communities. Annual Review of Microbiology, 75, 269–290. https://doi.org/10.1146/annurev-micro-031921-055801
- Sharan, M., Vijay, D., Dhaka, P., Bedi, J. S., & Gill, J. P. S. (2022). Biofilms as a microbial hazard in the food industry: A scoping review. *Journal of Applied Microbiology*, 133 (4), 2210–2234. https://doi.org/10.1111/jam.15766
- Sharma, S., Byrne, M., Perera, K. Y., Duffy, B., Jaiswal, A. K., & Jaiswal, S. (2023). Active film packaging based on bio-nanocomposite ${\rm TiO_2}$ and cinnamon essential oil for

- enhanced preservation of cheese quality. Food Chemistry, 405(Pt A), Article 134798. https://doi.org/10.1016/j.foodchem.2022.134798
- Shen, H., Durkin, D. P., Aiello, A., Diba, T., Lafleur, J., Zara, J. M., ... Shuai, D. (2021). Photocatalytic graphitic carbon nitride-chitosan composites for pathogenic biofilm control under visible light irradiation. *Journal of Hazardous Materials*, 408, Article 124890. https://doi.org/10.1016/j.jhazmat.2020.124890
- Sillankorva, S., Neubauer, P., & Azeredo, J. (2008). Pseudomonas fluorescens biofilms subjected to phage philBB-PF7A. BMC Biotechnology, 8, 79. https://doi.org/ 10.1186/1472-6750-8-79
- Simões, M., Pereira, M. O., Sillankorva, S., Azeredo, J., & Vieira, M. J. (2007). The effect of hydrodynamic conditions on the phenotype of Pseudomonas fluorescens biofilms. *Biofouling*, 23(3–4), 249–258. https://doi.org/10.1080/08927010701368476
- Singh, R., & Nalwa, H. S. (2011). Medical applications of nanoparticles in biological imaging, cell labeling, antimicrobial agents, and anticancer nanodrugs. *Journal of Biomedical Nanotechnology*, 7(4), 489–503. https://doi.org/10.1166/jbn.2011.1324
- Vorregaard, M. (2008). Comstat2—A modern 3D image analysis environment for biofilms, in informatics and mathematical modelling. Technical University of Denmark: Kongens Lyngby, Denmark. Kongens Lyngby, Denmark: Technical University of Denmark.

- Wagh, R. V., Priyadarshi, R., & Rhim, J.-W. (2023). Novel bacteriophage-based food packaging: An innovative food safety approach. *Coatings*, 13(3), 609. https://doi. org/10.3390/coatings13030609
- Wiguna, O. D., Waturangi, D. E., & Yogiara (2022). Bacteriophage DW-EC with the capability to destruct and inhibit biofilm formed by several pathogenic bacteria. Scientific Reports, 12(1), 18539. doi:https://doi.org/10.1038/s41598-022-22042-1.
- Xu, P., Chen, X., & Ren, H. (2024). Corrosion mechanisms of Escherichia coli and Pseudomonas fluorescens on carbon steel based on biofilm perspective. Corrosion Engineering, Science and Technology., 59(8), 552–571. https://doi.org/10.1177/ 1478422X241267363
- Xue, H., Feng, J., Zhang, K., Wang, Y., Liao, X., & Tan, J. (2025). Insights into the preparation, properties, application in food of polysaccharide-based edible films and coatings: An updated overview. Current Research in Food Science, 11, Article 101123. https://doi.org/10.1016/j.crfs.2025.101123
- Zegadło, K., Gieroń, M., Żarnowiec, P., Durlik-Popińska, K., Kręcisz, B., Kaca, W., & Czerwonka, G. (2023). Bacterial motility and its role in skin and wound infections. International Journal of Molecular Sciences, 24(2), 1707. https://doi.org/10.3390/ijms24021707